IOPscience iopscience.iop.org

Home Search Collections Journals About Contact us My IOPscience

Bonding structure and properties of ion enhanced reactive magnetron sputtered silicon carbonitride films

This article has been downloaded from IOPscience. Please scroll down to see the full text article.

2000 J. Phys.: Condens. Matter 12 L591

(http://iopscience.iop.org/0953-8984/12/37/101)

View the table of contents for this issue, or go to the journal homepage for more

Download details:
IP Address: 171.66.16.221
The article was downloaded on 16/05/2010 at 06:46

Please note that terms and conditions apply.

J. Phys.: Condens. Matter **12** (2000) L591–L597. Printed in the UK PII: S0953-8984(00)15767-4

LETTER TO THE EDITOR

Bonding structure and properties of ion enhanced reactive magnetron sputtered silicon carbonitride films

Xiao-Ming He, T N Taylor, R S Lillard, K C Walter and M Nastasi
Los Alamos National Laboratory, Los Alamos, New Mexico 87545, USA

Received 24 July 2000

Abstract. Amorphous silicon carbonitride (a-SiCN) films were synthesized by ion enhanced radio-frequency (rf) magnetron sputtering from a Si_4C target using a mixture of Ar and N_2 gases. The oxidation resistance of the films was investigated in an oxygen atmosphere over the temperature range of 0–1000 °C. X-ray photoelectron spectroscopy showed that the a-SiCN films exhibited a well-defined Si–C–N bonding structure. The composition, density, hardness, and stress were uniquely characterized with respect to the average energy per deposited atom. Under optimum deposition conditions a-SiCN films can be prepared to exhibit high density (>2.6 g cm^{-3}), high hardness (>25 GPa), and enhanced oxidization resistance at temperatures up to 800 °C.

Silicon carbonitride ceramics have received increasing interest in recent research due to their high hardness, enhanced oxidation and corrosion resistance compared to those of carbides and nitrides of silicon, and carbon nitride [1–5]. The enhancement of these properties has been attributed to complex-covalent chemical bonding and a low oxygen diffusion coefficient in the amorphous structure of the silicon carbonitride; excellent properties have been observed even at temperatures up to 1600 °C [1]. In most of the previous work silicon carbonitride has been synthesized in bulk using solution chemistry. Currently, silicon carbonitride or hydrogenated silicon carbonitride films have been synthesized with ion sputtering deposition of carbon and silicon in a nitrogen atmosphere [3], N^+ implantation into polycrystalline β-SiC [6], laser vapour phase reaction of hexamethyldisilazane (HMDS) with ammonia [7], chemical vapour deposition (CVD) and plasma-enhanced CVD using $Si(CH_3)_4$-NH_3-H_2, SiH_4-NH_3-CH_4, $(C_4H_9)_2SiH_2$-NH_3, or $Si_2NH(CH_3)_6$ atmospheres [2, 5, 8, 9]. Investigations have shown that different deposition methods led to the formation of silicon carbonitride films with amorphous or crystalline structures [4, 7, 10], while variations in the chemical composition of the films exhibited the dominant impact of bonding on structure and properties [2, 5, 11]. However, no detailed study on the properties, especially about the thermal stability and oxidation resistance of silicon carbonitride films, has yet been reported.

In this letter, we investigated the bonding structure and oxidation resistance of amorphous silicon carbonitride (a-SiCN) films prepared by ion enhanced magnetron sputtering. The average energy per deposited atom, E_{ave}, was uniquely used to evaluate the effects of the energy conditions of ion bombardment during deposition on the composition, density, hardness, and stress of the a-SiCN films. The a-SiCN films were deposited onto silicon (100) wafers, via reactive radio-frequency (rf) magnetron sputtering of a 4 inch diameter silicon carbide (Si_4C) target (99.99% purity) using a mixture of Ar and N_2 gases. The substrates were pre-cleaned ultrasonically in an acetone bath, rinsed in an ethanol bath, and then loaded into the deposition chamber. The base pressure in the chamber was $\leqslant 2.6 \times 10^{-6}$ Pa, and the working pressure, consisting of Ar and N_2 with a constant flow $F_{N2} + F_{Ar} = 60$ sccm, was set at 0.26 Pa. The

0953-8984/00/370591+07$30.00 © 2000 IOP Publishing Ltd

substrates were placed 10 cm away from the magnetron cathode and heated to 350 °C during all depositions. A direct-current (dc) pulsed negative bias, at a pulse width of 7 μs and a pulse frequency of 24 kHz, was applied on the sample stage to provide ion bombardment during the growth of the films. Prior to deposition, the substrates were sputter cleaned using parameters described in previous work [12]. In all experiments, the sputtering power density was kept at 3.8 W cm^{-2}. Two series of a-SiCN samples were prepared for this study. In the first series, the N_2 gas concentration was held at 25% and samples were made with different applied biases in the range between 0 and −550 V. In the second series, samples were made at a fixed bias of −250 V and the N_2 gas concentration was varied between 0 and 100%.

The synthesized a-SiCN films were visually very smooth and flat. No crystalline or grain features could be observed from the films under examination with SEM and TEM. Characterization of the atomic bonding was performed using x-ray photoelectron spectroscopy (XPS) and bremsstrahlung-excited Auger electron spectroscopy (AES) in an ESCA system (Model 5600ci, Physical Electronics, Eden Prairie, MN). Unfiltered Mg Kα radiation (1253.6 eV) was used as the excitation source. Spectra were acquired using a pass energy of 23.5 eV and a step interval of 0.05 eV. The bonding configuration of the a-SiCN film was compared to that of an amorphous silicon carbide (a-SiC) film and a crystalline Si_3N_4 powder. Figures 1(a), 1(b) and 1(c) show the Si2p, C1s, and N1s binding energy peaks (XPS) that were measured from a-SiCN (Si/C = 0.92 and N = 35 at.%), a-SiC (Si/C = 0.82 and N = 0%), and Si_3N_4. Before the measurements the a-SiCN and a-SiC samples were ion sputtered at 1000 eV for three minutes (20–30 Å removal) to eliminate any surface impurities adsorbed during air handling. The Si_3N_4 powder was analysed as-received with no sputtering. The spectra from the a-SiC and a-SiCN samples were not adjusted in energy with respect to an internal reference, but were irradiated by a neutralizing gun to eliminate any easily observable charge buildup while producing the highest quality lineshapes. The Si_3N_4 sample was referenced to the adventitious C 1s peak at 284.8 eV binding energy [13]. Because of the inherent uncertainties in the energy referencing due to sample charging, we do not emphasize the exact XPS and AES peak positions. Instead, we have circumvented this limitation for the Si component by measuring the Auger parameter, which is determined by measuring the energy difference between the Si 2p (XPS) and Si KLL (bremsstrahlung-excited AES) peaks. As the Auger parameter is an energy difference value, it is charge independent and uniquely defines the bonding configuration of the element under analysis [14].

The Si Auger parameters for the three samples are listed in figure 1(a). It was found that the Si KLL lineshapes for a-SiCN and a-SiC were similar to that for the Si_3N_4. However, the a-SiCN film has a value of 1715.10 eV, which lies midway between that of Si_3N_4 (1714.45 eV) and a-SiC (1716.05 eV). This is consistent with a Si electron configuration that has a bonding scheme involving both C and N, and is in agreement with the results published by Bendeddouche *et al* [5]. Further analysis of the XPS spectra shows that the full-width-at-half-maximum (FWHM) for the Si 2p peak from the a-SiCN is 2.1 eV, which is larger than that for the Si 2p peaks from both crystalline Si_3N_4 (1.79 eV) and a-SiC (1.84 eV). Similarly, figures 1(b) and 1(c) indicate that the FWHM of C 1s and N 1s peaks in a-SiCN is larger than the FWHM of those in Si_3N_4 and a-SiC. On the other hand, the N1s and C1s transitions from the a-SiCN film show an obvious asymmetry with a high binding energy contribution, compared to that for the Si_3N_4 (for N 1s) or the a-SiC (for C 1s). These higher binding energy states suggest the presence of N and C complexes that are somewhat peripheral to the Si bonding site in a-SiCN. The facts are correlated with the observation from the Si 2p peaks where the Si 2p energy of a-SiCN is higher than those of Si_3N_4 and a-SiC (see figure 1(a)). The high FWHM and high binding energy are attributed to the inter-bonded Si–C–N covalent structure that broadens the C 1s, N 1s, and Si 2p peaks in the a-SiCN film [3, 11]. Analysis of the XPS

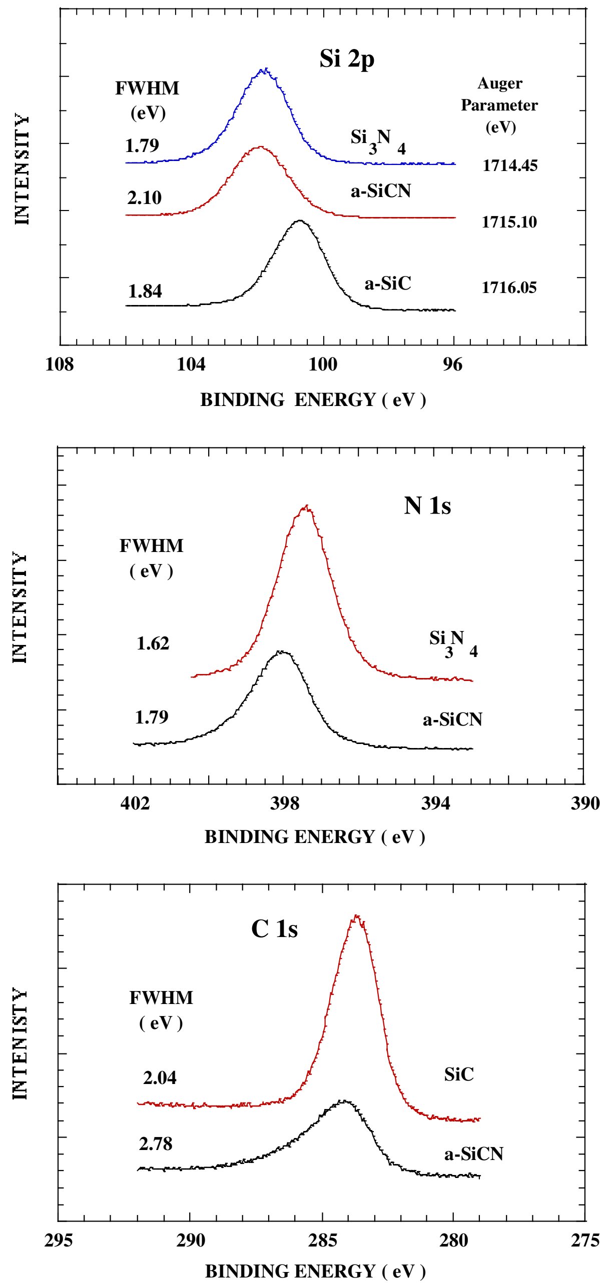

Figure 1. Typical XPS spectra of (a) Si 2p, (b) N 1s, and (c) C 1s binding peaks for the a-SiCN film, the a-SiC film, and the micro-crystalline Si_3N_4 powder.

spectra from other films with the compositions of Si/C = 0.83–1.1 and N = 32–38.2 at.% revealed a bonding configuration that is similar to that shown in figures 1(a), 1(b) and 1(c).

In ion enhanced deposition, the average energy per deposited atom has a dominant effect on the composition, structure and properties of the formed films [15]. The average energy can

be determined from the relationship [15]:

$$E_{ave} = E_{ion}(J_i/J_a) \quad (1)$$

where the average energy per deposited atom, E_{ave}, is directly determined by the bombarding ion energy (E_{ion}) and the arrival ratio of the bombarding ion flux (J_i) to the deposition atom flux (J_a), or J_i/J_a. The E_{ion}, however, is affected by the bias voltage (V_b) and the operating pressure (P) in the deposition chamber. The relationship between E_{ion} and V_b and P is given by the relationship [16]:

$$E_{ion} \approx k' V_b P^{-1/2} \quad (2)$$

where k' is a constant. In our process the pressure during deposition was 0.26 Pa and according to equation (2), the ion energy E_{ion} is nearly equal to the bias voltage times the electron charge [16]:

$$E_{ion} \approx eV_b. \quad (3)$$

In our analysis, we assumed that J_i arises mainly from ionized argon and nitrogen ions, while J_a consists of the sputtered Si and C atoms and the N atoms arriving at the sample surface. Assuming that the singly charged ions dominate the bombardment process, the time-averaged ion current density can be calculated by the approaches used in [17]. The value of J_a was calculated from RBS and RIBS measurements (see next paragraph) as the total number of deposited atoms per unit area divided by the deposition time. E_{ave} was calculated as a function of negative bias or N_2 gas concentration for all samples synthesized. It was found that the variation in the negative bias from 0 to −550 V resulted in an increase of E_{ave} from 0 to 260 eV while the adjustment of the N_2 gas concentration from 0 to 100% resulted in changes of E_{ave} from 70 to 167 eV.

The composition was analysed using Rutherford backscattering spectrometry (RBS) at 2 MeV $^4He^+$ to detect Si, and using resonant ion backscattering spectrometries (RIBS) at 5.6 MeV $^4He^{++}$ and 7.65 MeV $^4He^{++}$ to detect C and N, respectively [18]. The total number of atoms per cm^2 in the films and the film composition were obtained from the RBS and RIBS spectra by using the computer program RUMP [19]. The density of the films was then determined from the obtained atoms per cm^2 and the film thickness measured using a surface profilometer. In addition, the experimental methods and procedures used for the measurements of the hardness, elastic modulus, and stress of the a-SiCN films are the same with those in the previous work [12].

The composition, growth rate, density, hardness and stress of a-SiCN films are shown in figures 2(a), 2(b), and 2(c) as a function of the average energy per deposited atom, E_{ave}. The a-SiCN films were deposited at a constant N_2 gas concentration of 25% and with negative biases in the range of 0 to −550 V. It can be seen from figure 2(a) that increasing E_{ave} to 170 eV increases both the Si and N concentrations. Further increases in E_{ave} result in a continuous increase in Si while reducing the C and N concentrations. The increase of the Si/C ratio to above 0.92 is correlated with an increase in the film density to above 2.5 g cm^{-3} (figure 2(b)). However, the increase of E_{ave} results in a reduction of the deposition rate (figure 2(b)). This is most likely due to an increase in the amount of sputtering from the growing film with increasing E_{ave}. The hardness and stress data in figure 2(c) show that the a-SiCN films reach a maximum hardness of 25.5 GPa and a maximum compressive stress of −1.80 GP for E_{ave} in the range of 70–110 eV. Our observed hardness of $\sim$ 25 GPa is the highest value ever reported for a-SiCN to date [3, 9]. Further increases or reductions in E_{ion} result in the formation of a-SiCN films with stresses below 1.4 GPa and hardness below 22 GPa. Summarizing the data in figure 2, one can see that in the average energy range of 70–110 eV a-SiCN films grow at a high deposition rate (>0.17 nm s^{-1}) with chemical compositions of Si/C in the range of 0.92–0.94 and N 35 at.%

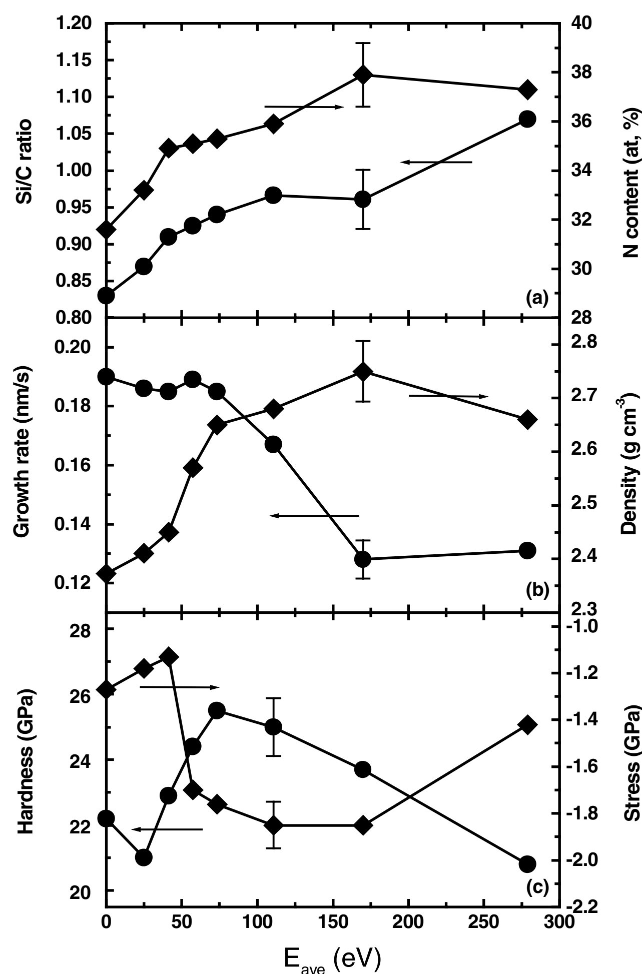

Figure 2. (a) Si/C atomic ratio and N concentration, (b) growth rate and mass density, and (c) hardness and residual stress of the a-SiCN films prepared at different average energy per deposited atoms. The deposition was performed at a pressure of 0.26 Pa, a N_2 gas concentration of 25%, and a negative bias voltage ranging from 0 to −550 V.

(or Si:N:C $\approx$ 1:1:1). The resultant a-SiCN films possess high hardness (>25 GPa) and high density (>2.6 g cm^{-3}).

Oxidation studies of the a-SiCN films were carried out at ambient pressure in a quartz cylinder tube furnace with an oxygen flow rate of 0.2 standard cubic feet per hour. The oxidation time was fixed at two hours at temperatures of 400, 600, 800 and 1000 °C. The chemical compositions of a-SiCN films after oxidation were measured using RBS and RIBS techniques. The a-SiCN films with a composition of 30.6 at.% Si, 33.3 at.% C and 35.0 at.% N, and a hardness of 24.5 GPa were used in all oxidation experiments. Figure 3 shows the RIBS spectra of the Si (100) substrate, as-deposited a-SiCN film, and a-SiCN films after oxidation at various temperatures. The random peaks in the spectra are from nuclear reactions with Si substrate. From these data, it can be seen that the RIBS spectrum from the 600 °C oxidized a-SiCN films totally overlaps the RIBS spectrum of the as-deposited a-SiCN film. However, following

an oxidation anneal at 1000 °C, an extra oxygen peak appears in RIBS spectra. Table 1 lists the results of the RUMP simulations, and the hardness and elastic modulus measurements on the a-SiCN films as a function of oxidation temperature. The data show that oxidation of the a-SiCN surface does not occur until the temperature is increased to 800 °C or higher. The oxide layer forms on the surface and has the composition of SiO_2. The oxide layer thickness increases from 108 to 260 nm with an increase in temperature from 800 to 1000 °C, which corresponds to an oxidation rate of 0.9 and 2.1 nm min^{-1} at 800 and 1000 °C, respectively. The RUMP simulations disclosed that there is a flat interface between the oxidized layer and the bulk a-SiCN films. In addition, the a-SiCN films maintain a high hardness above 20 GPa and elastic modulus above 170 GPa for oxidation anneals below 800 °C. The formation of a surface oxidation layer leads to an increase in the film thickness and a corresponding reduction in the hardness and elastic modulus. These changes in properties are especially pronounced for oxidation anneals at 1000 °C for two hours; the hardness and elastic modulus are reduced to 13 GPa and 130 GPa, which are slightly higher than the data of SiO_2 (hardness: 10 GPa, elastic modulus: 69.3 GPa).

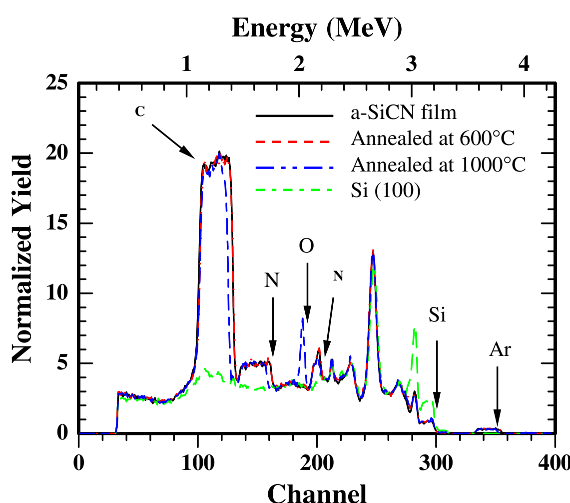

Figure 3. RIBS spectra of Si (100) wafer, as-deposited a-SiCN film, and a-SiCN films oxidized at temperatures of 600 and 1000 °C for 2 hours.

Table 1. The thickness of surface dioxide layer and the hardness and elastic modulus of a- SiCN films (film composition: O, 0.7 at.%; N, 35.0 at.%; Si, 30.6 at.%; C, 33.3 at.%; Ar, 0.4 at.%) oxidized at different temperatures.

Oxidation temperature (°C)	0	400	600	800	1000
Silicon dioxide layer (nm)	0	∼0	∼0	108	260
Hardness (GPa)	25	25	20–21	14–15	13
Elastic modulus (GPa)	220	200–210	170	150	130
Film thickness (μm)	∼1	∼1	∼1	∼1.1	1.18

In summary, ion enhanced magnetron sputtered a-SiCN films with compositions in the range of Si/C = 0.83–1.1 and N = 32–38.2 at.% have a low surface roughness and a well-defined Si–C–N bonding structure. The a-SiCN films formed with an average energy per deposited atom of 70–110 eV exhibit the chemical compositions of Si:C:N ≈ 1:1:1, a high

density (>2.65 g cm^{-3}), and a high hardness (>25 GPa). Oxidation studies of the a-SiCN films show that they are resistant to oxidation and maintain high hardness (>20 GPa) for anneals at temperature below 800 °C.

We acknowledge C Maggiore and J Tesmer for their technical support in these experiments. This work is supported by the Office of Basic Energy Science of the US Department of Energy.

References

[1] Riedl R, Kleebe H, Schonfelder H and Aldinger F 1995 *Nature* **374** 526
[2] Zhang W, Zhang K and Wang B 1994 *Mater. Sci. Eng.* B **26** 133
[3] He Z, Carter G and Colligon J S 1996 *Thin Solid Films* **283** 90
[4] Badzian A, Badzian T, Drawl W D and Roy R 1998 *Diamond Relat. Mater.* **7** 1519
[5] Bendeddouche A, Berjoan R, Beche E, Merle-Mejean T, Schamm S, Serin V, Taillades G, Pradel A and Hillel R 1997 *J. Appl. Phys.* **81** 6147
[6] Uslu C, Park B and Poker D B 1996 *J. Electron. Mater.* **25** 23
[7] Besling W F A, Goossens A, Meester B and Schoonman J 1998 *J. Appl. Phys.* **83** 544
[8] Fainer N I, Kosinova M L, Rumyantsev Y M and Kuznetson F A 1999 *J. Physique* **9** 8–769
[9] Levy R A, Grow J M, Yu Y and Shin K T 1995 *Mater. Lett.* **24** 47
[10] Chen L C, Yang C Y, Bhusari D M, Chen K H, Lin M C and Chuang T J 1996 *Diamond Relat. Mater.* **5** 514
[11] Gong Z, Wang E G, Xu G C and Chen Y 1999 *Thin Solid Films* **348** 114
[12] Xiao-Ming He, Baker N, Kehler B A, Walter K C, Nastasi M and Nakamura Y 2000 *J. Vac. Sci. Technol.* A **18** 30
[13] Moulder J F, Stickle W F, Sobol P E and Bomben K E 1992 *Handbook of X-Ray Photoelectron Spectroscopy, Physical Electronics Division, Perkin-Elmer, Eden Prairie, MN*
[14] Wagner C D, Gale L H and Raymond R H 1979 *Anal. Chem.* **51** 466
[15] Nastasi M, Mayer J W and Hirvonen J K 1996 *Ion-Solid Interactions: Fundamentals and applications* (Cambridge: Cambridge University Press) ch 13
[16] Robertson J 1992 *Surf. Coat. Technol.* **50** 185
[17] Lee D H, Walter K C and Nastasi M 1999 *J. Vac. Sci. Technol.* B **17** 818
[18] Tesmer J R and Nastasi M 1995 *Handbook of Modern Ion Beam Materials Analysis* (Copyright 1995 Materials Research Society, Printed in the USA) ch 6 and 7
[19] Doolittle L R 1985 *Nucl. Instrum. Meth.* B **9** 344
[20] Doolittle L R 1986 *Nucl. Instrum. Meth.* B **15** 227